The Polar Structures of $KNdNb_2O_7$ and $KNdTa_2O_7$.

Subhadip Mallick, Alexandra S. Gibbs, Weiguo Zhang, P. Shiv Halasyamani, Nicole A. Benedek*, and Michael A. Hayward*

Supporting Information

Table of Contents

1. Indexing of $KNdM_2O_7$ (M = Nb, Ta) phases.

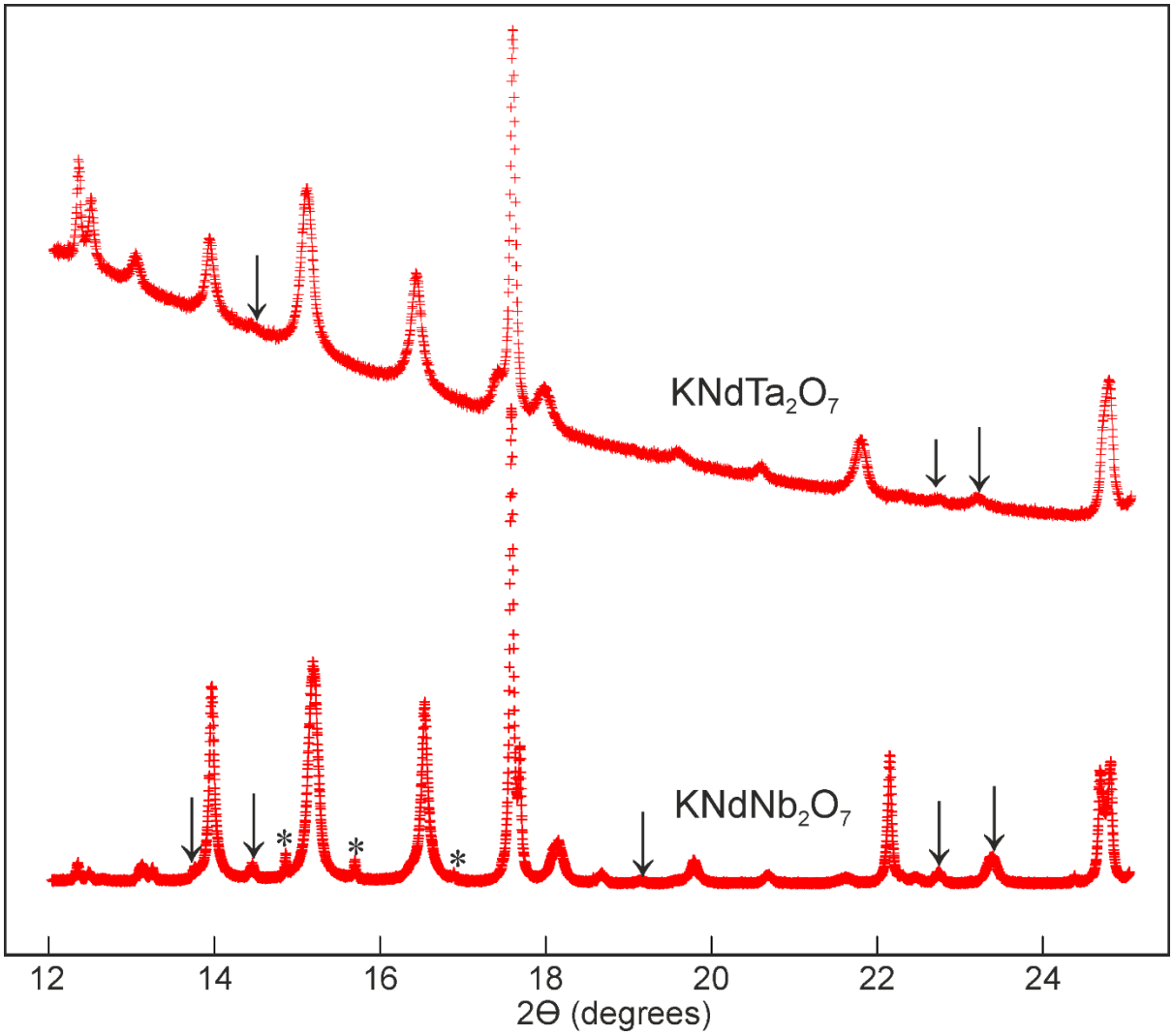

Figure S1. Synchrotron X-ray powder diffraction data collected from $KNdTa_2O_7$ and $KNdNb_2O_7$ in the range 12 <2θ (°) <25. Peaks indicated by the arrows denote the superlattice peaks attributed to (2, 0, 1) expansion of the aristotype unit cell. Asterisk marks indicate the peaks from a secondary phase $NdNbO_4$.

2. Symmetry Analysis of n = 2 (0, ½, z) structures

IRs	Glazer Tilt	Space Group	Lattice parameters
	$a^0b^0c^0$	*Ammm* (65)	*a , b, c*
Z1+	$a^0b^+c^0/\ a^0b^+c^0$	*Ammm* (65)	*a' = 2a, b' = b, c' = c*
T1+	$a^0b^+c^0/\ a^0(-b^+)c^0$	*Immm* (71)	*a' = b, b' = c, c' = 2a*
R2- (0;a	$a^0b^-c^0/\ a^0b^-c^0$	*C*2/*m* (12)	*a' = 2b, b' = 2a, c' = ½c*
R2- (a;b)	$a^0b^-c^0/\ a^0(-b^-)c^0$	*C*2/*m* (12)	*a' = 2b, b' = 2a, c' = c*
S1+ (0;a)	$a^+b^0c^0/\ a^+b^0c^0$	*P*2/*m* (10)	*a' = 2b, b' = a, c' = ½c*
S1+ (a;b)	$a^+b^0c^0/\ (-a^+)b^0c^0$	*P*2/*m* (10)	*a' = 2b, b' = a, c' = c*
R1- (0;a)	$a^-b^0c^0/\ a^-b^0c^0$	*C*2/*m* (12)	*a' = 2b, b' = 2a, c' = ½c*
R1- (a;b)	$a^-b^0c^0/\ (-a^0)b^0c^0$	*C*2/*m* (12)	*a' = 2b, b' = 2a, c' = c*
R1+ (0;a)	$a^0b^0c^+/\ a^0b^0c^+$	*C*2/*m* (12)	*a' = 2b, b' = 2a, c' = ½c*
R1+ (a;b)	$a^0b^0c^+/\ a^0b^0(-c^+)$	*C*2/*m* (12)	*a' = 2b, b' = 2a, c' = c*
S1+ • Z1+ (0;a|b)	$a^+b^+c^0$	*P*2/*m* (10)	*a' = 2b, b' = 2a, c' = ½c*
S1+ • Z1+ (a;b|c)	$a^+b^+c^0/(-a^+)b^+c^0$	*P*2/*m* (10)	*a' = 2b, b' = 2a, c' = ½c*
S1+ • T1+ (0;a|b)	$a^+b^+c^0/a^+(-b^+)c^0$	*C*2/*m* (12)	*a' = c, b' = 2a, c' = 2b*
S1+ • T1+ (a;b|c)	$a^+b^+c^0/-(a^+b^+)c^0$	*P*2/*m* (12)	*a' = 2b, b' = 2 a, c' = c*
R2- • R1- (0;a|0;b)	$a^-b^-c^0/a^-b^-c0$	*P*-1 (2)	*a' = √2a, b' = √2b, c' = ½c*
R2- • R1- (a;b|c;d)	$a^-b^-c^0/-(a^-b^-)c^0$	*P*-1 (2)	*a' = √2a, b' = √2b, c' = c*
R2- • R1- (0;a|b;0)	$a^-b^-c^0/(-a^-)b^-c^0$	*C*2/*c* (15)	*a' = 2b, b' = 2a, c' = c*
R1- • Z1+ (a|0;b)	$a^-b^+c^0/a^-b^+c^0$	*P*2/*c* (13)	*a' = ½c, b' = 2a, c' = 2b*
R1- • Z1+ (a|b;c)	$a^-b^+c^0/(-a^-)b^+c^0$	*P*2/*c* (13)	*a' = c, b' = 2a, c' = 2b*
R1- • T1+ (a|0;b)	$a^-b^+c^0/a^-(-b^+)c^0$	*C*2/*c* (15)	*a' = c, b' = 2a, c' = 2b*
R1- • T1+ (a|b;c)	$a^-b^+c^0/-(a^-b^+)c^0$	*P*2/*c* (13)	*a' = c, b' = 2a, c' = 2b*
R2- • S1+ (0;a|0;b)	$a^+b^-c^0/a^+b^-c^0$	$P2_1/m$ (11)	*a' = 2b, b' = 2a, c' = ½c*
R2- • S1+ (a;b|c;d)	$a^+b^-c^0/-(a^+b^-)c^0$	$P2_1/m$ (11)	*a' = 2b, b' = 2a, c' = c*
R2- • S1+ (0;a|b;0)	$a^+b^-c^0/a^+(-b^-)c^0$	*C*2/*m* (12)	*a' = c, b' = 2a, c' = 2b*

Table S1. 'Chemically plausible' distortions of the n = 2 (0, ½, z) stacked perovskite structure. The first column describes the irreducible representations for each distortion (labels as for the *Ammm* space group). The second column lists the Glazer-tilt description of the distortions. Column 3 lists the space-group of the distorted structure, and column 4 the unit cell expansion relative to the *Ammm* aristotype structure.

3. Comparison of *Immm* vs *Ammm* indexing.

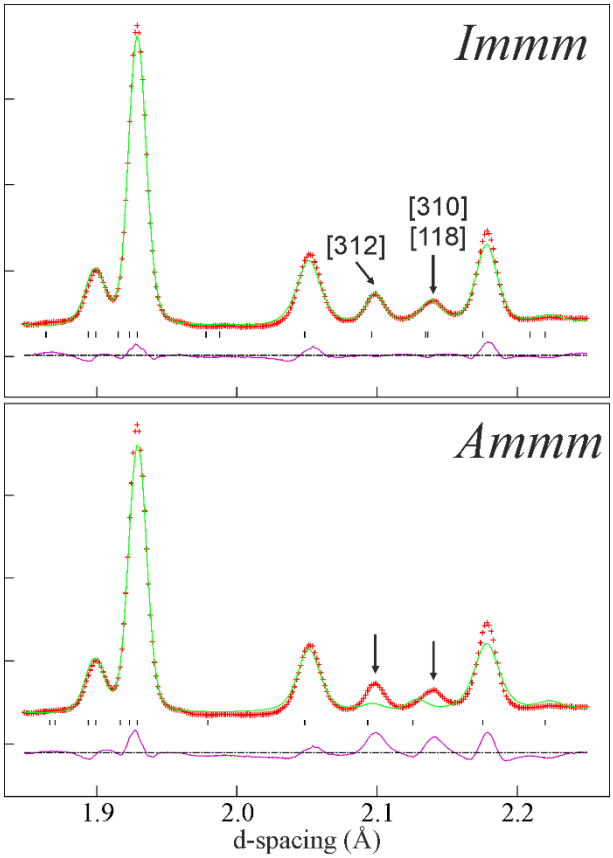

Figure S2. Observed, calculated and difference plots from the refinement of structural models in space groups *Ammm* and *Immm* against powder neutron diffraction collected from $KNdTa_2O_7$. Arrows indicate systematically absent [312] and [310]/[118] reflections in the space group *Ammm*.

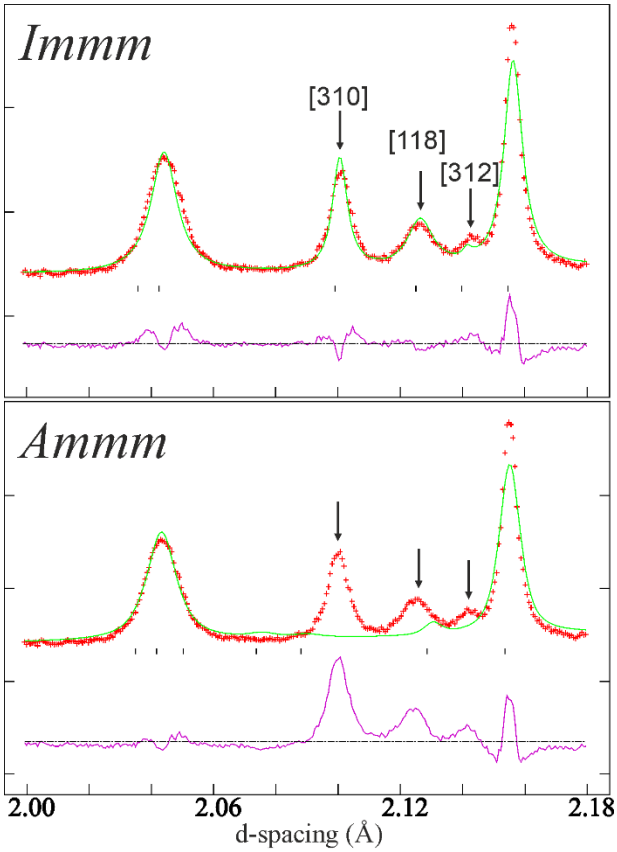

Figure S3. Observed, calculated and difference plots from the refinement of structural models in space groups *Ammm* and *Immm* against powder neutron diffraction collected from $KNdNb_2O_7$. Arrows indicate systematically absent [312] and [310]/[118] reflections in the space group *Ammm*.

4. Comparison of *Immm*, *Im*2*m* and *I*222 models.

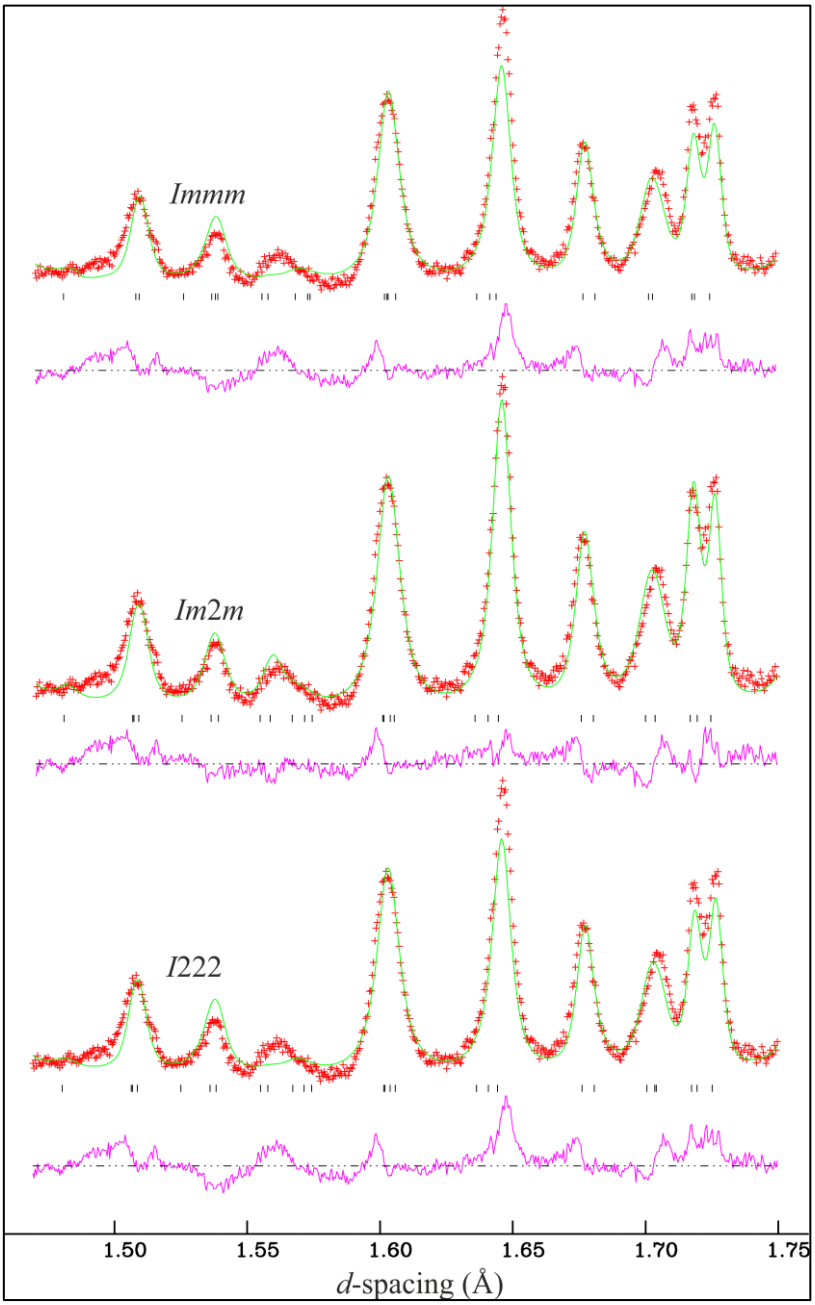

Figure S4. Observed, calculated and difference plots from the structural refinement of models described in the space groups *Immm*, *Im*2*m* and *I*222 space against the neutron powder diffraction data collected from $KNdTa_2O_7$.

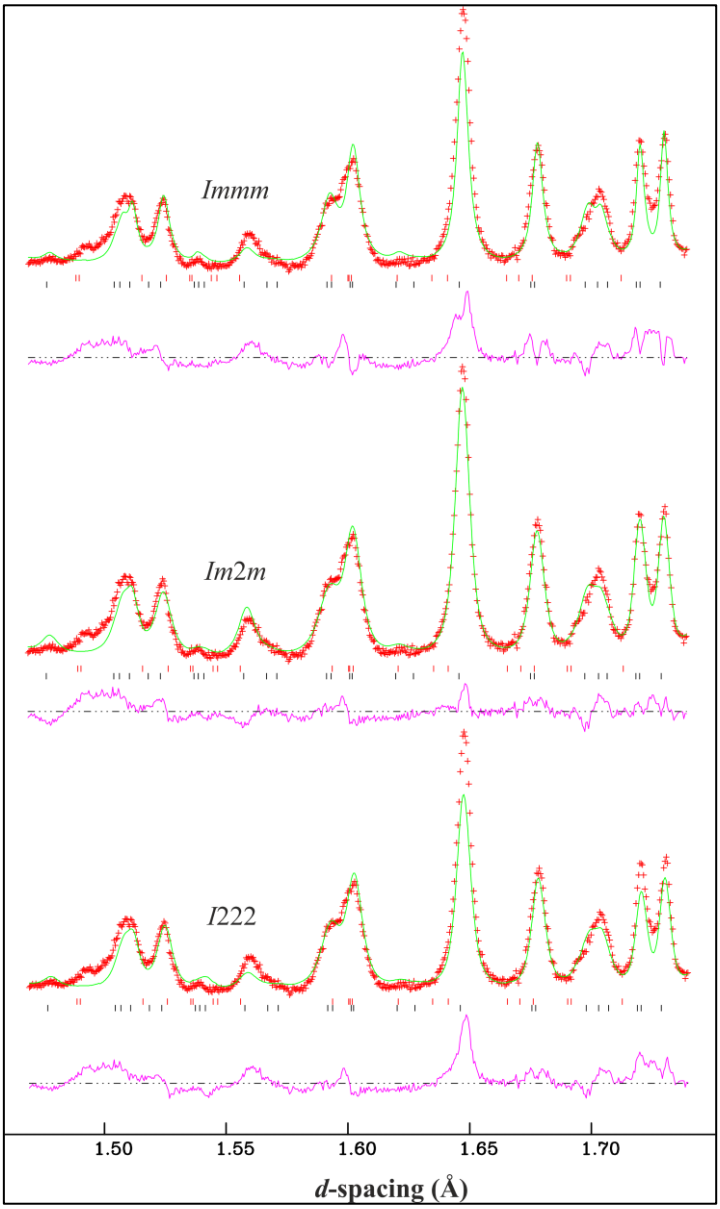

Figure S5. Observed, calculated and difference plots from the structural refinement of models described in the space groups *Immm*, *Im*2*m* and *I*222 space against the neutron powder diffraction data collected from $KNdNb_2O_7$. $NdNbO_4$ was added as a secondary phase, as indicated by red tick marks.

5. Refined structures $KNdM_2O_7$ (M = Nb, Ta) phases.

Atom	Label	Site	*x*	*y*	*z*	Occ.	U_{iso} (Å^2)
K	K1	4*c*	0	0.0074(37)	0.2354(4)	1	0.0036(19)
Nd	Nd1	2*a*	0	0.0182(36)	0	1	0.0176(22)
	Nd2	2*b*	0.5	0.0405(27)	0	1	0.0110(19)
Ta	Ta1	8*e*	0.7516(5)	0.0194(11)	0.3992(1)	1	0.0041(5)
O	O1	4*d*	0.2812(6)	0.5869(14)	0	1	0.0104(17)
	O2	4*c*	0	0.1071(16)	0.4076(2)	1	0.0007(15)
	O3	4*c*	0	0.5570(23)	0.9224(2)	1	0.0094(15)
	O4	8*e*	0.7169(5)	0.0196(21)	0.3174(1)	1	0.0251(11)
	O5	8*e*	0.7457(11)	0.0294(24)	0.0831(1)	1	0.0508(12)
$KNdTa_2O_7$ – space group *Im*2*m* (#44)							
a = 7.7018(6) Å, b = 3.8613(3) Å, c = 21.7688(17) Å, volume = 647.37(14) Å^3							
Formula weight = 657.23 g mol^{-1}, Z = 4							
Radiation source: Neutron Time of Flight							
Temperature: 298 K							
χ^2 = 28.26, R_p = 5.50 %, $_wR_p$ = 5.94 %							

Table S2. Parameters from the structural refinement of $KNdTa_2O_7$ against neutron powder diffraction data collected at 298 K.

Cation	Anion	Bond length (Å)	BVS
K 1	O4 × 2	2.768(13)	K +0.97
	O4 × 2	2.818(7)	
	O4 × 2	2.833(13)	
Nd 1	O1 × 2	2.732(10)	Nd+2.67
	O1 × 2	3.084(12)	
	O3 × 2	2.455(13)	
	O3 × 2	2.680(14)	
	O5 × 4	2.667(7)	
Nd 2	O1 × 2	2.431(10)	Nd+3.02
	O1 × 2	2.700(10)	
	O2 × 2	2.617(9)	
	O2 × 2	2.972(10)	
	O5 × 4	2.618(8)	
Ta 1	O1	2.221(3)	Ta+5.29
	O2	1.951(5)	
	O3	2.008(5)	
	O4	1.801(4)	
	O5	1.931(11)	
	O5	2.007(11)	

Table S3. Selected bond lengths from the refined structure of $KNdTa_2O_7$.

Atom	Label	Site	*X*	*y*	*z*	Occ.	U_{iso} (Å^2)
K	K1	4*c*	0	0.0078(38)	0.2371(4)	1	0.0175(22)
Nd	Nd1	2*a*	0	0.0123(29)	0	1	0.0122(18)
	Nd2	2*b*	0.5	0.0113(25)	0	1	0.0136(18)
Nb	Nb1	8*e*	0.7515(5)	0.0230(10)	0.3985(1)	1	0.0034(5)
O	O1	4*d*	0.2862(6)	0.5934(13)	0	1	0.0125(17)
	O2	4*c*	0	0.1073(14)	0.4020(2)	1	0.0134(18)
	O3	4*c*	0	0.5254(25)	0.9267(2)	1	0.0095(12)
	O4	8*e*	0.7160(4)	0.0411(18)	0.3180(2)	1	0.0219(10)
	O5	8*e*	0.7617(9)	0.0408(24)	0.0856(2)	1	0.0445(11)
$KNdNb_2O_7$ – space group *Im*2*m* (#44)							
a = 7.7093(5) Å, b = 3.8709(2) Å, c = 21.5558(16) Å, volume = 643.28(13) Å^3							
Formula weight = 481.14 g mol^{-1}, Z = 4							
Radiation source: Neutron Time of Flight							
Temperature: 298 K							
χ^2 = 38.88, R_p = 6.61%, $_wR_p$ = 6.70 %							

Table S4. Parameters from the structural refinement of $KNdNb_2O_7$ against neutron powder diffraction data collected at 298 K.

Cation	Anion	Bond length (Å)	BVS
K 1	O4 × 2	2.729(12)	K+0.97
	O4 × 2	2.802(7)	
	O4 × 2	2.906(13)	
Nd 1	O1 × 2	2.738(9)	Nd+2.89
	O1 × 2	3.151(10)	
	O3 × 2	2.459(12)	
	O3 × 2	2.538(12)	
	O5 × 4	2.606(6)	
Nd 2	O1 × 2	2.309(9)	Nd+2.99
	O1 × 2	2.792(10)	
	O2 × 2	2.628(8)	
	O2 × 2	3.128(9)	
	O5 × 4	2.736(6)	
Nb 1	O1	2.221(3)	Nb+5.32
	O2	1.945(4)	
	O3	2.032(4)	
	O4	1.758(5)	
	O5	1.900(10)	
	O5	2.036(10)	

Table S5. Selected bond lengths from the refined structure of $KNdNb_2O_7$.

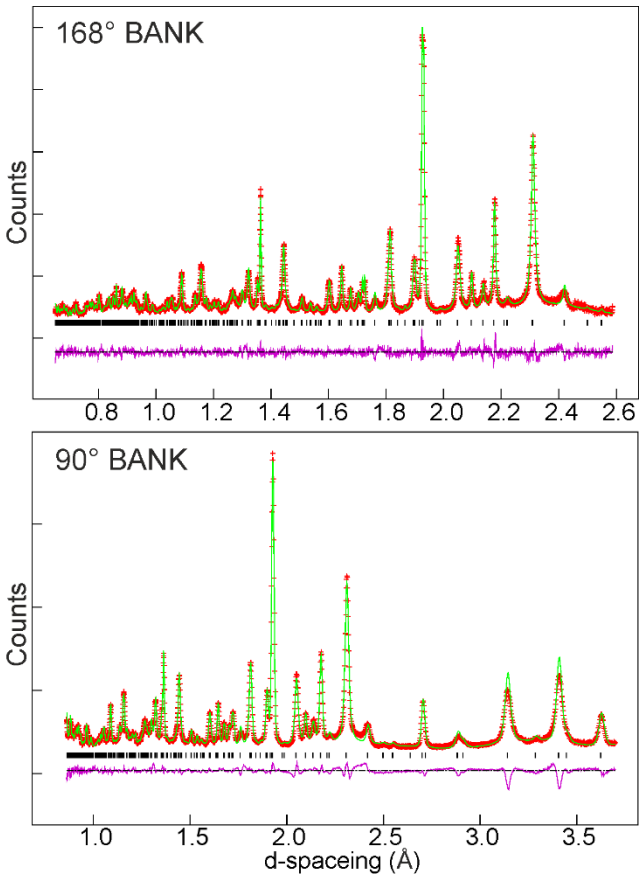

Figure S6. Observed, calculated and difference plots from the structural refinement of $KNdTa_2O_7$ against neutron diffraction data.

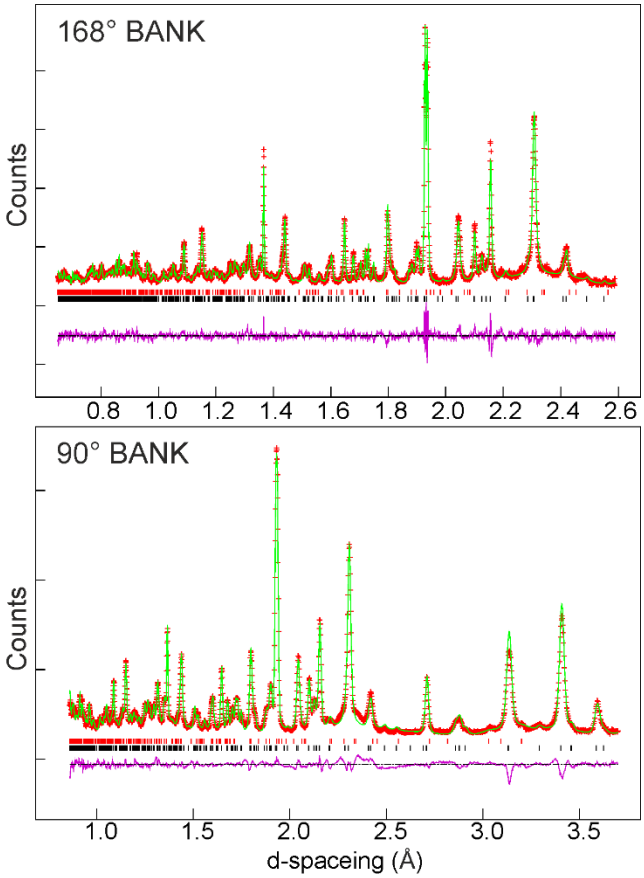

Figure S7. Observed, calculated and difference plots from the structural refinement of $KNdNb_2O_7$ against neutron diffraction data. Lower tick marks indicate peak positions for the majority phase, upper tick marks for an $NdNbO_4$ secondary phase.

6. First-Principles Analysis of the $KNdNb_2O_7$.

Atom	Label	Site	*x*	*y*	*z*
K	K1	4*c*	0.00000	0.02927	0.24197
Nd	Nd1	2*a*	0.00000	0.02943	0.00000
Nd	Nd2	2*b*	0.50000	0.02918	0.00000
Nb	Nb1	8*e*	0.74740	0.02932	0.39670
O	O1	4*d*	0.30363	0.52928	0.00000
O	O2	4*c*	0.00000	0.02958	0.39303
O	O3	4*c*	0.00000	0.52943	0.93025
O	O4	8*e*	0.70075	0.02926	0.31486
O	O5	8*e*	0.75684	0.02936	0.08193
KNdNb2O7 – space group *Im2m* (#44) *a* = 7.7127 Å, *b* = 3.9052 Å, *c* = 21.2133 Å					

Table S6. Parameters from the energy minimized structure of $KNdNb_2O_7$.

7. Analysis of the tilting distortions of $KNdM_2O_7$ (*M* = Nb, Ta) phases.

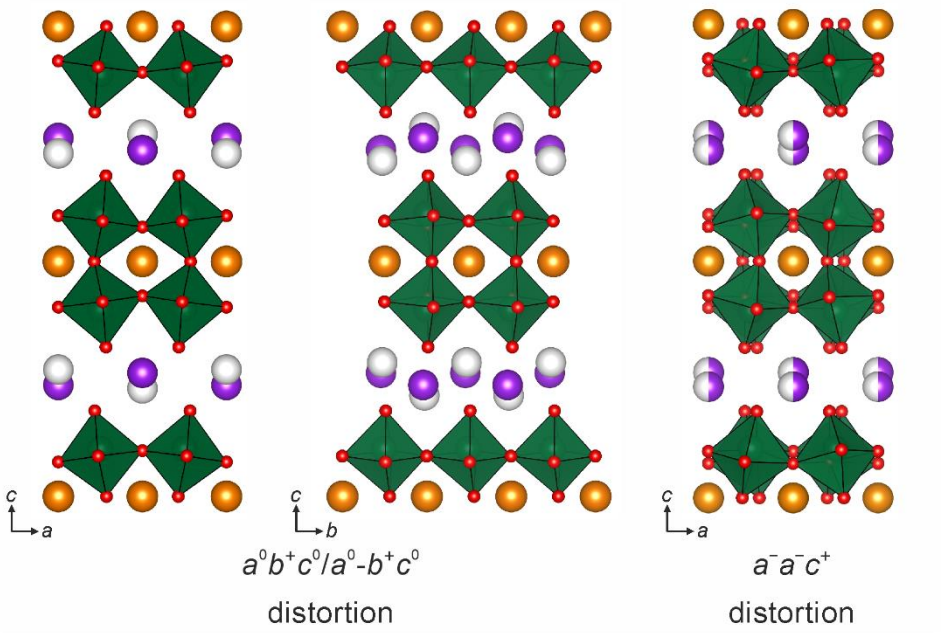

Figure S8. Observed, $a^0b^+c^0/a^0$-b^+c^0 distorted structure of $KNdNb_2O_7$ (left) and hypothetical $a^-a^-c^+$. distorted structure (right). Green, orange, red, purple and grey spheres represent Nb, Nd, O, K and K-vacancies respectively. Half-shading of the K ions indicates a disordered 50% occupation in the $a^-a^-c^+$ distorted model.

8. Analysis of the M^{5+} cation off-centering distortions of $KNdM_2O_7$ (M = Nb, Ta) phases.

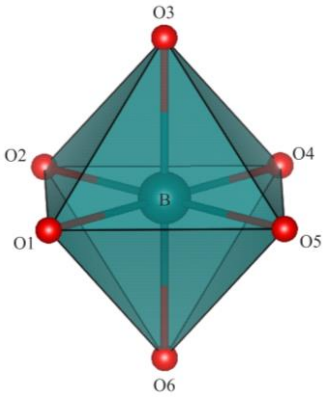

Above is a regular BO_6 octahedron. The magnitude of the off-center distortion can be quantified by considering the <*B*-O> bond lengths and the deviation from the linearity of the three *trans* ∠O-*B*-O bond angles. If we define the *trans* bond angles as θ1 = ∠O1-*B*-O4, θ2 = ∠O2-*B*-O5 and θ3 = ∠O3-*B*-O6; the magnitude of out of center distortion, $\Delta_d = (|< B-O1 > - < B-O4 >| \div |cos\,\theta 1|) + (|< B-O2 > - < B-O5 >| \div |cos\,\theta 2|) + (|< B-O3 > - < B-O6 >| \div |cos\,\theta 3|)$. A non-zero value will be obtained if the *B*-cation is off-centered. Using the *Im*2*m* structural models refined against neutron diffraction data (Tables S2 - S5), we obtain Δ_d = 0.569 and 0.709 for $KNdTa_2O_7$ and $KNdNb_2O_7$ respectively.